Accepted Manuscript

Quantitative methods for compensation of matrix effects and self-absorption in LIBS signals of solids

Tomoko Takahashi, Blair Thornton

PII: S0584-8547(16)30329-9
DOI: doi:10.1016/j.sab.2017.09.010
Reference: SAB 5303

To appear in: *Spectrochimica Acta Part B: Atomic Spectroscopy*

Received date: 28 February 2017
Revised date: 13 September 2017
Accepted date: 13 September 2017

Please cite this article as: Tomoko Takahashi, Blair Thornton, Quantitative methods for compensation of matrix effects and self-absorption in LIBS signals of solids, *Spectrochimica Acta Part B: Atomic Spectroscopy* (2017), doi:10.1016/j.sab.2017.09.010

This is a PDF file of an unedited manuscript that has been accepted for publication. As a service to our customers we are providing this early version of the manuscript. The manuscript will undergo copyediting, typesetting, and review of the resulting proof before it is published in its final form. Please note that during the production process errors may be discovered which could affect the content, and all legal disclaimers that apply to the journal pertain.

ACCEPTED MANUSCRIPT

Quantitative methods for compensation of matrix effects and self-absorption in LIBS signals of solids

Tomoko Takahashi[a], Blair Thornton[a,b]

[a] *Institute of Industrial Science, The University of Tokyo, 4-6-1, Komaba, Meguro, Tokyo 153-8505, Japan*
[b] *Southampton Marine and Maritime Institute, University of Southampton, Burgess Road, Southampton SO16 7QF, UK*

Abstract

This paper reviews methods to compensate for matrix effects and self-absorption during quantitative analysis of compositions of solids measured using Laser Induced Breakdown Spectroscopy (LIBS) and their applications to in-situ analysis. Methods to reduce matrix and self-absorption effects on calibration curves are first introduced. The conditions where calibration curves are applicable to quantification of compositions of solid samples and their limitations are discussed. While calibration-free LIBS (CF-LIBS), which corrects matrix effects theoretically based on the Boltzmann distribution law and Saha equation, has been applied in a number of studies, requirements need to be satisfied for the calculation of chemical compositions to be valid. Also, peaks of all elements contained in the target need to be detected, which is a bottleneck for in-situ analysis of unknown materials. Multivariate analysis techniques are gaining momentum in LIBS analysis. Among the available techniques, principal component regression (PCR) analysis and partial least squares (PLS) regression analysis, which can extract related information to compositions from all spectral data, are widely established methods and have been applied to various fields including in-situ applications in air and for planetary explorations. Artificial neural networks (ANNs), where non-linear effects can be modelled, have also been investigated as a quantitative method and its application is introduced. The ability to make quantitative estimates based on LIBS signals is seen as a key element for the technique to gain wider acceptance as an analytical method, especially in in-

ACCEPTED MANUSCRIPT

situ applications. In order to accelerate this process, it is recommended that the accuracy should be described using common figures of merit which express the overall normalised accuracy, such as the normalised root mean square errors (NRMSE), when comparing the accuracy obtained from different setups and analytical methods.

Keywords: Laser induced breakdown spectroscopy (LIBS), Quantitative analysis, Matrix effect, Self-absorption

1. Introduction

Laser Induced Breakdown Spectroscopy (LIBS) is a form of atomic emission spectroscopy that requires no sample preparation, makes rapid measurements, and delivers results in near real-time. Since laser ablated materials from which optical emissions occur are in the form of atoms and ions, elemental analysis of targets in the solid, liquid, and gaseous phases is possible. Both its versatility and ease of use have led to the application of LIBS to in-situ elemental analysis. In particular, LIBS has great potential for in-situ analysis of solid targets since techniques capable of doing this are limited. The accuracy of solid measurements using LIBS is often compared to X-ray fluorescence analysis (XRF), which can also measure elements in solid targets on site. Considering the overall accuracy, it can be said that the suitability of LIBS for in-situ analysis is comparable to XRF [1]. The application fields of LIBS are rapidly expanding, with geological [2], archaeological [3], and industrial [4] measurements. Field measurements have also been performed in various environments with lightweight and compact systems [5], such as in nuclear power plants [6], on other planets [7] and in deep-sea environments [8, 9]. In particular, LIBS has a great advantage in application to aquatic environments, since XRF suffers from significant attenuation of X rays in water. While it has been reported that well-resolved emission lines from solids submerged in water can be obtained using a double-pulse LIBS [10], the enhancement of signals cannot be observed under high pressure [11, 12, 13, 14]. Based on the work of Sakka et al. [15] and Thornton et al. [16],

ACCEPTED MANUSCRIPT

which demonstrated signal enhancement for solids submerged in water at high pressure using a long ns-duration pulse (> 100 ns), metallic elements in natural hydrothermal deposits were successfully measured in situ at depths over 1000 m on the seafloor [8].

One of the fundamental challenges for in-situ analysis using LIBS is quantification of elemental compositions. It has often been reported that conventional calibration curves suffer from matrix effects [17, 18]. Matrix effects occur due to different reasons. The spectral matrix effect occurs when strong lines of a matrix element interfere with weak lines of an analyte element. This can be avoided by careful peak selection or peak fitting. Correction of matrix effects due to different physical characteristics and chemical compounds is more challenging than the spectral matrix effect. The physical matrix effect depends on the physical property differences of samples, e. g., heat of vaporization, thermal conductivity, absorption coefficient, water content of samples, which affect the transport of an ablated mass into plasma. The chemical matrix effect occurs when the presence and density of a matrix element affect the emission characteristics of an analyte element due to the ionisation tendency and compound form [19]. Since natural targets such as rocks and soils are diverse, preparation of matrix matched standards for in-situ applications is not practical [20]. In addition, self-absorbed spectral lines show non-linear response of peak heights with their concentrations. Self-absorption occurs due to the energy difference for the excitation levels of atoms that exists at high density in the plasma, resulting in flat-topped spectral lines, or a dip in the center (self-reversed) [21]. Therefore these effects need to be compensated for during the analysis. In this paper, quantitative analytical methods for compensation of matrix effects and self-absorption for solid targets are reviewed. The traditional calibration curve based approaches are discussed in Chapter 3, calibration-free LIBS (CF-LIBS) is discussed in Chapter 4, and multivariate analyses such as principal component regression analysis (PCR), partial-least squares regression analysis (PLSR, PLS), and artificial neural networks (ANNs), are discussed in Chapter 5. In each chapter, the methods and their applications are described, especially focusing

ACCEPTED MANUSCRIPT

on the results of in-situ analysis.

2. Figures of merit

A calibration curve is a linear regression model of known concentrations as a function of peak intensities regarding a certain element. The accuracy of linear fitting is often evaluated by a correlation coefficient R or a coefficient of determination R^2 of the calibration curve. The uncertainty of the model can be visualised by drawing confidence and prediction bands on the calibration curves [22]. The accuracy of the concentration calculation is often represented by drawing a linear regression model of known concentrations as a function of calculated concentrations in many works (for example, [23, 24, 25]). In the ideal case, the linear model should be $y = \hat{y}$, where y and $\hat{y}$ represent the predicted and reference concentration, respectively. The accuracy of the model is evaluated based on the slope, y-intercept and R or R^2 values of the estimated linear model. Absolute errors (AEs) and relative errors (REs, in %) are widely used to determine the prediction accuracy [26, 27]:

$$\begin{aligned} \text{AE} &= |\hat{y} - y| \\ \text{RE} &= |\frac{\hat{y} - y}{\hat{y}}| \times 100. \end{aligned} \tag{1}$$

While an AE is a direct indicator of error, samples with low concentrations typically have small values of AEs. On the other hand, RE values can be very large for samples with low concentrations, especially when approaching the limit of detection (LOD). When convergence of data of each sample is discussed, the standard deviation (SD), or more commonly SD of the population (σ) is used to describe the amount of deviation of data given as:

$$\text{SD} = \sqrt{\frac{\sum_{i=1}^{N_d}(y_i - \overline{y})^2}{N_d}} \tag{2}$$

$$\sigma = \sqrt{\frac{\sum_{i=1}^{N_d}(y_i - \overline{y})^2}{N_d - 1}}. \tag{3}$$

ACCEPTED MANUSCRIPT

where $\overline{y}$ represents the mean value of predicted concentrations y_i over the N_d datasets. The relative standard deviation (RSD in %), is also a common figure of merit [28, 29] given as:

$$\mathrm{RSD} = \frac{\mathrm{SD}}{\overline{y}} \times 100. \tag{4}$$

However, these values are used to describe the error within datasets of one sample and do not indicate the overall accuracy of the calibration. Several values are introduced to indicate the overall accuracy of concentration estimation. The average RE of prediction (REP in %) is often used [30, 31]:

$$\mathrm{REP} = \frac{1}{N}\sum_{i=1}^{N}\mathrm{RE}_i \tag{5}$$

where RE_i indicates the RE of sample i over the N samples. It should be noted that components of low concentrations have inherently large REs, since the value is divided by the known concentration. Tognoni et al. [32] proposed the value distance, which is the summation of AEs, to compensate for this problem:

$$\mathrm{distance} = \sum_{i=1}^{N}\mathrm{AE}_i \tag{6}$$

where AE_i indicates the AE of sample i over the N samples. The mean square error (MSE) and root MSE (RMSE) can also describe the overall accuracy of all sample datasets. MSE and RMSE represent the deviation of the predicted values from the reference values:

$$\begin{aligned} \mathrm{RMSE} &= \sqrt{\mathrm{MSE}} \\ \textit{where}\quad \mathrm{MSE} &= \frac{\sum_{i=1}^{N}(\hat{y}_i - y_i)^2}{N}. \end{aligned} \tag{7}$$

The unit of RMSE is the same as the unit of reference and predicted concentrations. RMSE is referred to as RMSEC for calibration data, RMSEP for prediction data, and RMSECV for cross-validation data. These values are often used for evaluation of the accuracy when multivariate analysis is applied. Since RMSE depends on the range of concentrations, normalised RMSE is also used [33]:

$$\mathrm{NRMSE} = \frac{\mathrm{RMSE}}{y_{\max} - y_{\min}} \tag{8}$$

ACCEPTED MANUSCRIPT

where $y_{\max}$ and $y_{\min}$ represent maximum and minimum concentrations in the dataset. Predicted residual error sum of squares (PRESS) is the sum of AEs:

$$\mathrm{PRESS} = \sum_{i=1}^{N} {\mathrm{AE}_i}^2. \tag{9}$$

It should be noted that the value of PRESS depends on the total number of samples and the range of concentrations. It is often used for evaluation of the optimal number of principal components (PCs) and latent variables (LVs) in cross validation for PCR and PLS analysis, respectively. However, due to its dependence on the composition of the dataset used, PRESS cannot be used as a general indicator for comparison between different datasets.

Results can be discussed from multi perspectives using different figures of merit. However, it should be noted that certain common figures of merit should be used when accuracy of results obtained from different experimental setups and methods is compared.

3. Studies on calibration curves

3.1. Basic calibration curves

Calibration curves have been successfully applied to quantitative analysis of iron ore [34], soils in air [18, 35], and metals submerged in water using a double-pulse LIBS technique [13] with matrix matched standards. However, the applications are limited to specific elements. For example, only Mn and Si of iron ore samples were measured using calibration curves in Ref. [34]. Grant et al. [36] reported that systematic overestimation was seen in calibration curves of Al and Ti for ore samples, stating that this might be because of matrix effects. In general, matrix effects need to be taken into account for calibration curves [37, 38, 39]. Chemical matrix effects on minor elements in rock samples were thoroughly investigated using samples doped with Cr, Mn, Ni, Zn, and Co measured in Mars-like atmospheric environments [40]. Through analysis of 175 samples with 5 different matrices, the authors concluded that spectral line selection without interference of neighbouring lines is an important factor and

ACCEPTED MANUSCRIPT

sample matrices should be similar to draw accurate calibration curves. As for line selection, another paper reported that although some carbon emission lines interfere with iron lines in soil samples, calibration curves with an accuracy of R = 0.91 for cross validation can be obtained with particular emission lines [41]. It can be said that suitable lines for calibration curves exist and can be determined by preliminary analysis. As for the sample matrix, prior knowledge about a target sample is necessary to construct a sample database with similar matrices, which is often difficult for in-situ analysis. In order to select appropriate samples without prior knowledge of sample matrix types, Pořízka et al. [25] applied principal component analysis (PCA) for data clustering to find similarities in signal sets and drew calibration curves of Cu in soil samples grouped by PCA with $R^2 = 0.95$.

Experimental conditions, such as laser and detector parameters, can also affect the accuracy of calibration curves. Rosenwasser et al. [42] developed a method in which spectral lines with minimum interference from other elements and optimal experimental parameters such as laser energy, gate delay and width of a detector are selected automatically. Under these conditions, the compositions of P, Al, Ca, Mg and Si in ore samples could be determined by calibration curves with $R > 0.98$ and RSD = 2-4 %. In addition, the physical condition of the samples were found to influence the results. Anzano et al. [43] investigated the effect of sample preparation for Fe and Al in ore samples, and found that signals from powder-form samples are not affected by matrix effects that affect pressed pellets. From these studies, it should be noticed that the application of calibration curves to absolute quantification is limited to specific cases due to matrix effects.

3.2. Normalisation

It is known that normalisation of the peak intensity of an analyte element by a matrix element can diminish the effect of shot-to-shot fluctuations of signals due to experimental conditions [28] as well as the chemical matrix effect [23]. There are several examples of calibration curves where the ratio of an element

ACCEPTED MANUSCRIPT

and a reference element (matrix element) are used. In this case, changes in the amount of material ablated due to physical properties, e. g., differences between heat of vaporization, thermal conductivity, are assumed to be constant when the ratio of elements is considered. This method is referred to as internal standard normalisation, and it is effective when the concentration of a reference element is known. The criteria to choose a reference line are described as follows [44, 45]:

- the reference and analyte line should be close and should lie in the spectrum collected by the same detector,
- the analyte and reference lines should be independent of other lines in order to avoid spectral matrix effects,
- the intensity of the reference line should be one to two orders of magnitude larger than the analyte line,
- ionization and excitation energies, volatilization rates, and atomic weights of analyte and reference lines should be comparable, and
- the line should not have any self-absorption (reduction of the observed peak intensity) due to high density of the species at the lower energy level [21, 46].

Using this method, Eppler et al. [18] formulated an accurate calibration curve for Pb/Fe. Harmon et al. [47] successfully formulated a calibration curve for Pb/Mg as a function of Pb concentrations for soil samples. In order to increase the reliability of calculation, Vrenegor et al. [48] suggested an inter element correction method, in which the effects of multiple reference elements on a peak of a certain element can be considered by introducing the "multiplicative factor", and showed a reduction in RMSE of up to 24 %. As for underwater LIBS, the calibration curves of element ratios have been applied to metals [12, 29] and sediments [49] ablated using a double-pulse or sequential double-pulse technique. Sallé et al. [50] compared internal standard normalisation with external standard normalisation in which a peak is normalised by the same peak seen in

ACCEPTED MANUSCRIPT

a reference sample. These were also compared with CF-LIBS, concluding that the external standard normalisation had the highest accuracy among internal and external standard normalisation, and CF-LIBS. While the external standard normalisation requires matrix matched samples, a relatively small number of samples is sufficient unlike conventional calibration curves and it is applicable to in-situ analysis under the condition where test samples with the similar matrix to a target can be measured in the same environment. While normalisation by peak intensity can reduce matrix effects in many instances, some targets still are affected by strong matrix effects, such as brass alloys due to the difference of changes in the mass ablation rate [51].

Methods to correct chemical matrix effects due to differences between emission properties such as ionization levels, normalisation by plasma parameters are also proposed in some studies. Chaléard et al. [52] used a function in which excitation temperatures (hereafter temperatures) and vaporized mass are taken into account for normalisation, and calibration curves with $R^2 > 0.99$ were obtained for Cu and Mn. Xu et al. [53] normalised the peak intensity by the intensity of the continuum, which is proportional to electron number density. The normalisation of emission intensities by surface densities of materials was proposed in Ref. [54], and quantified Mg concentrations in organic and inorganic samples with an accuracy of up to 25 %. Panne et al. [55] observed the same trends in fluctuations of peak intensities and temperature, and showed improvement in the accuracy of calibration curves by normalising the intensities of Mg I and II lines by temperature in addition to internal standard normalisation, where reference lines of Si I, Ca II, Al I were used.

Appropriate selection of reference lines can be used to construct reliable calibration models. Other parameters regarding plasma emission can be used for normalisation when a reference element is not available. However, non-linear effects due to self-absorbed spectral lines are still problematic, and methods to correct self-absorption are described in the next subsection.

ACCEPTED MANUSCRIPT

3.3. Self-absorption correction

While Davies et al. [56] applied internal standard normalisation to remote LIBS and measured the relative concentrations of trace elements to iron in steel samples, non-linear effects were still seen due to self-absorption at higher concentrations. The self-absorption effect, even if it is not obviously seen in the shape of the line, can affect the accuracy of calibration curves [36, 57, 58]. Since self-absorption is often seen in strong lines emitted from atoms and ions which relax back to their ground state, lines which terminate at higher energy levels can be selected as analytical lines since the effects of self-absorption are reduced. The downside of this is that the number of useful analytical lines for calibration curves can become limited, and higher temperatures are required [36]. Self-absorption can be corrected using a theoretical model of an optically thick plasma. This can be modelled using the concept of curve-of-growth (COG) [37]. Gornushkin et al. [59] first applied COG to a Cr peak and analysed the characteristics of laser-induced plasma such as temperature and the number density through COG. The experimental data successfully fitted the theoretical COG model, which expressed the difference of relations between the peak intensities and concentrations for a broad range of concentrations. Aragón et al. [60] extended COG to several Fe lines having different optical depths and degrees of self-absorption and confirmed that COG can be applied to lines with different optical thicknesses. The same group [61] also applied COG not only to lines from neutral atoms but also ionic emission lines, concluding that for both neutral and ionic emission lines, heavily self-absorbed lines cannot be corrected using COG. Other solutions are the modelling of lines for estimation of the self-absorption coefficient to obtain the theoretical intensity of lines that are strongly self-absorbed. Kuzuya et al. [62] calculated a theoretical intensity from the intensity of Cu lines where self-absorption is obviously seen using a physical model proposed in Ref. [63], and demonstrated that their method was effective for generating calibration curves with a high degree of linearity for the ratio of Cu/Si intensities as a function of Cu concentrations. Lazic et al. [64] calculated concentrations of different elements (Zn, Ni, Na, Mn, Mg, Fe, Cr,

ACCEPTED MANUSCRIPT

Ca, Ba and Al) in marine sediments through theoretical plasma modelling including optically thick plasma and self-absorption, with a RE within 20 % for most elements.

The self-absorption coefficient can be also experimentally determined by comparing two line profiles taken with and without a mirror located behind the plasma, and self-absorption effects can be successfully corrected [65]. When the self-absorption coefficient can be determined precisely, it is possible to significantly increase the accuracy of the calculation of elemental compositions using calibration curves [66].

These studies are essential to understand the mechanism of plasma emission in LIBS, which is complex and dynamic, and many methods to reduce matrix effects and correct self-absorption have been proposed to improve the accuracy of calibration curves. However, it is possible that the effectiveness of these methods is dependent on the specific elements (samples) and experimental conditions used. Quantitative analysis of samples with complex compositions such as natural rocks is still hampered by the strong matrix effects, and generic methods independent of sample properties and matrix are required especially for in-situ analysis of unknown targets where matrix matched standards cannot be prepared.

4. CF-LIBS

4.1. Method

CF-LIBS has been introduced by Ciucci et. al [67] to determine chemical composition without the need for calibration curves, by accounting for physical and chemical matrix effects theoretically through analysis of the spectrum. A review of CF-LIBS has been published in Ref. [68]. Here we introduce the basic idea of CF-LIBS calculations but do not describe the method in detail. In CF-LIBS, based on the Boltzmann distribution law (eq. 10) and Saha equation (eq. 11) when the electron number density is considered, the concentration of an element is calculated from its peak heights and parameters regarding each

ACCEPTED MANUSCRIPT

peak, the temperature and electron number density.

$$\ln\frac{I_{s_{ij}}}{A_{s_{ij}}g_{s_i}} = -\frac{E_{s_i}}{k_{\mathrm{B}}T} + \ln\frac{FN_s}{U_s(T)}, \tag{10}$$

$$N_{\mathrm{e}}\frac{{N_s}^{\mathrm{II}}}{{N_s}^{\mathrm{I}}} = \frac{(2\pi m_{\mathrm{e}}k_{\mathrm{B}}T)^{3/2}}{h^3}\frac{2{U_s}^{\mathrm{II}}(T)}{{U_s}^{\mathrm{I}}(T)}e^{-E_{s_{\mathrm{ion}}}/k_{\mathrm{B}}T}, \tag{11}$$

where $I_{s_{ij}}$ is the intensity of the spectral line in arbitrary units, $A_{s_{ij}}$ is the transition probability (s^{-1}), g_{s_i} is the statistical weight, E_{s_i} is the excitation energy (eV), k_{B} is the Boltzmann constant (eV K^{-1}), T is the temperature (K), F is an experimental parameter that takes into account the optical efficiency of the observing system, the plasma density and volume, N_s is the number density of each emitted species, $U_s(T)$ is the partition function, ${N_s}^{\mathrm{I}}$ and ${N_s}^{\mathrm{II}}$ are the number densities of the neutral atomic species and the singly ionized species (cm^{-3}), respectively, $E_{s_{\mathrm{ion}}}$ is the ionization potential of each neutral species in its ground state (eV), m_{e} is the electron mass (eV m^{-2} s^2), and h is the Planck constant (eV s). The subscripts i, j and s indicate the upper energy level i and lower energy level j of the element s. In order to calculate the temperature, the Boltzmann distribution law (eq. 10) is used to plot the intensity and spectral information of lines of different excitation energies that are emitted from the same element. The gradient of the Boltzmann plot can be used to determine the temperature. The electron number density can be determined from the Stark broadening effect on emission lines, assuming that other sources of broadening are negligible or can be compensated for [37].

In order to apply the Boltzmann distribution law and Saha equation, the following assumptions need to be satisfied [68];

- local thermal equilibrium (LTE) is satisfied,
- no self-absorption takes place (spectral lines in the calculation are optically thin),
- the plasma is considered as a spatially homogeneous source, and
- ablation is stoichiometric.

ACCEPTED MANUSCRIPT

It should be examined whether these assumptions are satisfied for each experimental condition. While the LTE condition is traditionally determined using the McWhirter criterion [69], it has been reported that the McWhirter criterion alone is not sufficient to conclude that LTE conditions are satisfied and additional criteria such as parameters regarding the relaxation time and variation length in the plasma are required [17, 70]. LTE can be realized by selecting the optimal time delay and gate width. Self-absorption is problematic for CF-LIBS as well as calibration curves and so lines without self-absorption or corrected lines should be used for calculations. The conditions of plasma homogeneity and stoichiometric ablation are difficult to control and generally need to be assumed from obtained results [71], while it is possible to limit the effects on CF-LIBS results under specific experimental conditions.

Differences in the chemical and physical properties of the target cause matrix effects that affect the emitting species within the plasma. The parameters in the Boltzmann distribution law and Saha equation express these to compensate for any effects within the plasma itself, and this is representative of the target under the assumption of stoichiometric ablation. While several peaks of the same element with different excitation levels need to be observed in the spectrum for calculation of temperature and information of spectral lines is necessary, the whole process is performed using only information about the peaks without large numbers of spectra for construction of a calibration model. This point is an advantage for in-situ applications as well, since no preparation of a calibration model is required.

So far, a number of studies measuring various kinds of targets using CF-LIBS have been published, investigating its application to metals [72, 73, 74, 75, 76], oxides [26], geological samples [77] including rocks and soils in an extraterrestrial atmospheric conditions [78], paintings [79], and organic materials [80, 81, 82, 83]. In the next subsections, CF-LIBS application case studies are reported discussing the fulfilment of the assumptions, correction of self-absorption and uncertainty of parameters in the calculation.

ACCEPTED MANUSCRIPT

4.2. Failure of assumptions

CF-LIBS is a powerful tool for quantification of elements under the conditions when the necessary assumptions are satisfied. Assuming that the plasma is in the LTE condition, Corsi et al. [38] compared CF-LIBS to calibration curves for quantification of Au, Ag, and Cu in precious alloys. In their work, possible causes of variability in experimental data and the uncertainty in the temperature were found to have little effect on the accuracy of CF-LIBS calculations, and showed the advantage of CF-LIBS for taking into account matrix effects. Shah et al. [72] succeeded in quantification of Fe, Cr, Ni, Mn and Si in steel alloys with RE < 5 % by optimising time delays so that the plasma is in LTE and optically thin.

It should be noted, however, that in practical scenarios failure of assumptions is often reported. The types of failure are summarized in Ref. [32]. As for the LTE condition, it has been reported that non-metallic elements tend to show non-LTE condition more often than metallic elements [70]. However, since the condition of LTE can be checked as described in the previous subsection, the experimental conditions can be optimised so that the spectrum for CF-LIBS calculation is taken within an observation time window when LTE is satisfied. Therefore, it can be said that the failure of LTE is not a critical problem.

Spatial inhomogeneity of plasma leads to inaccuracy of the calculation of temperature and electron density since the only one representative temperature and electron density are determined using the Saha-Boltzmann method. These inaccuracy directly leads to miscalculation of compositions. While it is possible to create almost uniform plasma in a controlled environment such as in argon, temperature and electron density of the peripheral plasma zone were found to be significantly lower than those of the core zone regarding the plasma created in air [84, 85, 86]. Dynamic changes in the difference of temperatures between zones were also seen among different matrices and delay times [87]. The difference of temperature and electron density within the plasma was found to lead a significant accuracy decrease of CF-LIBS results for minor elements by a simulation-based approach [88]. However, Gornushkin et al. also reported in

ACCEPTED MANUSCRIPT

the same reference that the 1 % REs were obtained for iron with the concentration of 98.9 % even from non-uniform plasmas, which suggests that CF-LIBS is applicable to quantitative analysis of major elements. It is also suggested by Hermann et al. [84] that the effect of plasma inhomogeneity on CF-LIBS results would be limited if only transitions of small optical thickness are considered, since the peripheral zone contributes to the plasma emission spectrum by absorption. In addition, it is possible to observe the early stage of a plasma where inhomogeneity is not significantly seen yet, with a gated detector, such as an intensified charge coupled device. Therefore, it can be said that the effect of spatial inhomogeneity on CF-LIBS results can be limited by suitable experimental conditions and peak selection.

It is suggested in the reference that the effect of plasma inhomogeneity on CF-LIBS results would be limited if only transitions of small optical thickness are considered, since the peripheral zone contributes to the plasma emission spectrum by absorption.

Non-stoichiometric ablation can take place for samples containing elements with large differences in their physical properties. Under these conditions, the results of matrix correction in CF-LIBS, which represents the ablated elements in the plasma, are not representative of the concentration of elements in the sample. Fornarini et al. [73] reported that elements in copper based alloys cannot be accurately quantified using CF-LIBS due to the differences in the physical properties of metal constituents. This nonstoichiometric phenomenon is often reported for brass samples in laser-ablated plasmas [89], and it was found through simulation that Zn is mainly responsible for plasma nonstoichiometry. Discrepancies between values calculated using CF-LIBS and the actual composition were also observed due to nonstoichiometric ablation in Refs. [46, 73, 90]. Lednev and Pershin [90] suggested a corrected CF-LIBS (CCF-LIBS) approach in which the preferential evaporation of different elements are considered. Having said this, under some experimental conditions, stoichiometry of the plasma generated from brass samples can be satisfied in atmospheric [75] and underwater environments [91], and further investigations are necessary to assess the

ACCEPTED MANUSCRIPT

effect of different laser irradiation, environmental, sample surface and detector gating conditions on stoichiometric ablation.

4.3. Self-absorption correction

The effects of self-absorption are seen in the results of CF-LIBS. In particular, self-absorbed lines tend to have lower intensities than the theory suggests, and this affects the accuracy of the temperature calculation. While one solution is to use only peaks without self-absorption in the calculation, strong lines which are emitted from a transition to the ground energy level are prone to self-absorption, and limiting the number of peaks can lead to less reliable calculations of temperature in CF-LIBS. The correction methods introduced in section 3, such as the COG method, can also be applied to CF-LIBS [92]. The C-sigma approach, which was recently proposed by Aragón and Aguilera [93] generalises the COG method for multiple lines emitted by different elements in the same ionization state. Using the C-sigma approach, the reliability of temperature calculation is significantly improved. The C-sigma approach was further applied to absolute quantitative analysis of Fe, Ca and Mn in fused glass samples with concentrations in the order of 100-200 ppm [94]. The concentrations were calculated with 9 % average REs while higher REs were observed especially in Ca, possibly due to matrix effects. It should be noted, however, that one of the advantages of CF-LIBS is that the processes can be completed without preparing reference samples. Methods which can directly correct self-absorption from analysis only using the LIBS spectrum have also been reported. The intensities of self-absorbed lines can be corrected using an internal reference line whose coefficient of self-absorption can be obtained [95]. Amamou et al. [96] expressed the degree of self-absorption directly using parameters of spectral lines including transition probabilities in the presence of self-absorption for Gaussian and Lorentzian shapes under the assumption of a homogeneous plasma in LTE. The theoretical results were consistent with experimental results. ElSherbini et al. [97] also developed an evaluation method to calculate self-absorption coefficients for both atomic and ionic emission lines of aluminum, which is also applied to

ACCEPTED MANUSCRIPT

emission lines of other elements [98]. While the method requires several reference lines without self-absorption, the further study found that intensities of one reference line at different temperatures obtained from several spectra are enough for determination of the self-absorption coefficient [99]. These works have led to improvement of the precision in temperature determination.

4.4. Uncertainty of parameters in the Boltzmann distribution law

Other possible causes which lead to inaccurate calculations of concentrations are experimental aberrations, accuracy of spectral data, and uncertainties in the parameters of equations. Herrera et al. [75] and Sallé et al. [50] analysed the possibility of CF-LIBS for metal alloys in the atmospheric environment and for geological samples in the Martian environment, respectively. Considering the accuracy obtained, which was REs of 5-20 % for metal alloys and REs of 1-190 % for geological samples, it was concluded that CF-LIBS can be used as a semi-quantitative method. Possible reasons for the unsatisfactory accuracy are explained by uncertainty in the knowledge of spectroscopic parameters such as the transition probabilities and the partition function used in the Boltzmann distribution law, or intensity fluctuations. Intensity fluctuations and the errors in temperature determination can lead to large errors in concentration calculations using CF-LIBS. Tognoni et al. [74] investigated the expected precision and accuracy of CF-LIBS, and the relative concentrations of the major elements were determined by ± 1 % variability, while concentrations of minor elements varied within ± 150-200 % under a simulation of temperature dispersion and large intensity fluctuations. From the results, it was concluded that spectra reproducibility is a major factor that influences CF-LIBS accuracy. Recently, methods which can take these uncertainties into account using a single matrix-matched standard have been proposed. Gaudiuso et al. [100] determined suitable temperatures from the known composition of one standard sample by carrying out the inverse calculation of CF-LIBS. The temperature can be determined accurately by considering the variation of calculated temperature differences among elements, and using this value of temperature, the

ACCEPTED MANUSCRIPT

compositions of other samples were calculated. A similar concept has been proposed in one-point calibration LIBS (OPC-LIBS) [101]. This approach also uses one matrix-matched standard, which is used to determine a function to correct for the variation in parameters. The advantages of OPC-LIBS are that it does not require detailed analysis of plasma conditions, and that self-absorption can be corrected if it occurs to a similar degree for the calibration standard and the unknown samples. Using OPC-LIBS, the accuracy of the CF-LIBS calculation improves significantly, from REs of 24-692 % determined by traditional calibration curves to 0-100 % [101]. However, the underlying assumption is that the temperature of a single sample is the representative of the remaining samples measured under the same condition, and so it is yet to be confirmed to what extent these methods can be applied in cases where the target composition and matrices vary significantly.

4.5. In-situ applications

For in-situ applications in which complex and unknown samples such as soils and rocks are measured, the application of CF-LIBS can be limited by the requirement of detection of peaks from all elements contained in a target [75, 50, 102]. The major elements in soils and rocks, such as K and S, are difficult to detect in typical experimental conditions, and only relative concentrations of detected elements could be compared in Ref. [75]. However, this can be useful in geological applications since it allows concentration ratios, not signal intensity ones, to be determined.

5. Multivariate regression analysis

5.1. PCR and PLS

5.1.1. Method

Multivariate regression analysis can construct a calibration model using all spectral and compositional data, by correlating spectral data with known composition changes [103]. In multivariate regression analysis, spectral datasets of

ACCEPTED MANUSCRIPT

samples with known compositions need to be prepared for a training dataset. The concentrations of unknown samples in a test dataset can be calculated using the calibration model constructed by the training dataset. On the assumption that chemical and physical matrix effects are expressed in spectral intensities and shapes of matrix element peaks, multivariate regression analysis considers the effects by constructing a statistical model using information in the full spectra of all samples in a database. While not meeting the required plasma conditions and uncertainties in parameters can lead to inaccurate estimates using CF-LIBS, multivariate regression can find information in the spectra that is related to concentration calculations when constructing the model, without the need for prior assumptions of the plasma condition. In addition, since multivariate regression methods can find any kind of input to output relationship, it can also be used to infer information regarding elements where the concentrations are known in the training data, even if there are no related peaks in the original spectra. It should be noted that this can only yield meaningful results if there exists a systematic relationship with a surrogate element or combination of elements that do exhibit peaks in the spectra.

PCR and PLS are the most common methods for multivariate regression analysis used in LIBS. Both methods can take into account chemical and physical matrix effects by including peak information of matrix elements in the model as with other multivariate regression analysis. In addition, effects of random noise, spectral matrix and self-absorption can be theoretically diminished by eliminating spectral information which shows redundancy or non-linear response to the analyte concentrations using a derived feature space. While PCs are extracted only from signal information in PCR, PLS takes into account both signal and elemental concentrations in extracting LVs from the original signal data. Detailed methods for calibration using PCR and PLS can be found in several articles (for example, [104, 105, 106]). One of the strengths of PCR and PLS among multivariate regression analyses is that the performance can be examined by extracted regression coefficients, which are the PCs and LVs. A drawback of some of multivariate regression analyses such as ANNs is that the

ACCEPTED MANUSCRIPT

constructed model is "a black box", in which information regarding the relationships that are used by the model remains unknown. A major risk of this is that data can be overfitted by the model. From this point of view, PCR and PLS are less prone to over-fitting since the relationships identified by the model can be expressed and visually confirmed using loading curves. Nonetheless, since the over-fitting problem can still exist, calibration models should be examined by cross-validation or validation models in order to examine existence of the problem for all multivariate techniques.

However, although PCR and PLS can decrease the effects of random noise and non-linear systematic effects in the signals on quantitative results by extracting PCs and LVs, these methods cannot include the effects in the model. Therefore, extremely strong variations in the degree of self-absorption cannot be modelled accurately using PCR or PLS and would result in large uncertainties for all predictions.

5.1.2. Model construction, correction of matrix effects and self-absorption

Quantification of elements using PCR and PLS can be quickly performed without detailed information or analysis of each peak, or even identification of peaks. It should be noted that when models are trained on a limited range of compositions, prediction performance is poor for extrapolating outside the training range, which is also a typical problem for conventional calibration curves [28]. Therefore, in order to make a robust and reliable calibration model, samples with various matrices should be used for model construction. Especially, for samples with complex matrices, such as geological samples, samples which particular elements are doped artificially do not increase variation of the matrices in the model, and so samples with originally different matrices should be used for model construction [107]. It should be noted, however, that in some cases the prediction accuracy of individual samples need to be compromised in order to get the best overall accuracy for a model when constructed using samples with a broad range of concentrations. In order to overcome the limitations of calibration and prediction using a single model, Anderson et al. [108] recently

ACCEPTED MANUSCRIPT

proposed the sub-model approach where the composition of the unknown target is predicted using the suitable sub-model determined by the estimated composition of the target using a full model, and found that the sub-model approach had lower RMSEP than conventional PLS.

In one of the early works regarding the use of PLS in LIBS, Amador-Hernandez et al. [109] applied PLS1 to quantify Au and Ag in Au-Ag-Cu alloys for analysis of jewellery samples. In this case, the optimal spectra were those where the continuum was removed not by time-resolved observation but by background correction, which increases the signal-to-noise ratios. In addition, the spectral range where less strong resonance lines are observed is preferred since less self-absorption occurs. While selection of peaks without self-absorption or optimisation of experimental conditions are typical in multivariate analysis, PCR and PLS can be adapted to reduce the influence of self-absorbed lines, that deviate from the linear relation, by weighting the region less than other regions of the spectra. Death et al. [107] observed this in their work on quantitative analysis of iron ore samples using PCR when other non self-absorbed lines were also observed in the regions. However, when self-absorbed lines are clearly seen and dominant in the region, the results were less accurate [110]. When the observable spectral regions are limited to ones where self-absorbed lines are dominant, it is possible to apply methods of self-absorption correction introduced in calibration curves and CF-LIBS, although it is not common to input spectral information after correction of self-absorption to PCR or PLS models. While there exist many methods for correction of self-absorption, and even some of which can be automated, detailed analysis of the peaks is required and this often assumes some prior knowledge of the target, which is not necessarily the case in field applications where multivariate techniques are popular. However, when correction can be performed, it can be expected that combination with PCR or PLS will lead to improvement of the accuracy.

From these studies, it can be said that while it is ideal to prepare a large number of samples with wide variation of matrix types and compositions as much as possible for model construction, in reality, preliminary analysis depend-

ACCEPTED MANUSCRIPT

ing on targets and elements is required to determine the optimal experimental conditions, sample variation and signal processing methods.

5.2. ANN

5.2.1. Method

An ANN is a non-linear machine learning technique [20, 111]. ANNs are now widely accepted in many fields such as finance, data mining and computer vision [112, 113] and have been applied in analytical chemistry as well [114]. With regard to regression analysis, the strength of ANNs among other multivariate analysis methods is that any relation between the spectra and elemental concentrations, regardless of linearity or non-linearity, can be described in the model. ANNs can statistically model patterns between input and output data that cannot be easily described by other methods, by having a high-degree of flexibility and handling a large amount of data [111]. As with other multivariate methods, the model does not account for causes and effects, and so the effects of both systematic and random processes are modelled altogether in one bulk complex model that is automatically constructed to best explain the correlation between the spectral intensity inputs and the known elemental concentrations of samples in the database. Therefore, any process that disturbs the linear relation between concentrations and intensities, such as any kinds of matrix effects including spectral, chemical, and physical effects, self-absorption, continuum, background noise, and signal fluctuations can be incorporated into the model as long as the patterns are sufficient repeatable across the training data, whereas in linear methods they would be accounted for as uncertainties. A number of textbooks describing the details of ANNs have been published [111, 115]. Fig. 1 shows the concept of a feedforward ANN. Hidden layers are introduced between the input and output layers. As input data passes through each layer, components of the signals are strengthened, weakened or cancelled by different values of weights, biases, and an active function which each node has. Since there is no systematic rule to determine the parameters regarding hidden layers such as the number of layers and nodes, weights, biases, and active functions of

ACCEPTED MANUSCRIPT

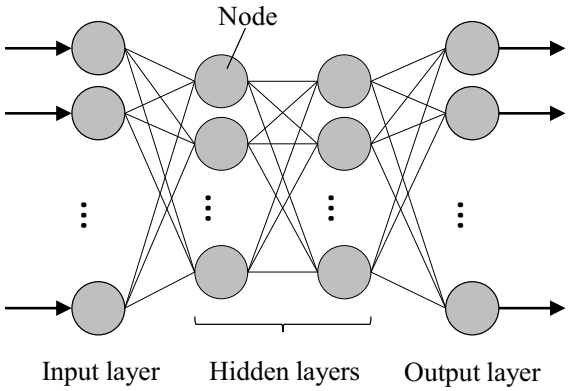

Figure 1: Simple framework of an artificial neural network.

nodes, these parameters are usually determined by finding parameters that give the best fit to the available training data through a number of trials.

It should be noted, however, that while ANNs have an advantage in expressing non-linear relations between concentrations and signals, it is difficult to confirm that the model is optimised or be assured that the regression model will be valid when applied to measurements of unknown samples. Unlike PCs or LVs for PCR or PLS, it is not possible to interpret the regression model visually and ANNs typically require a large database to train the model. As a result, efforts in optimisation using a particular database with ANNs are more prone to overfitting, where the prediction error can become larger than the calibration error.

5.2.2. Model construction, correction of matrix effects and self-absorption

One of the motivations to apply ANN to quantitative analysis for LIBS is that it can include non-linearity with a high-degree of flexibility, which can pose

ACCEPTED MANUSCRIPT

an advantage for modelling complex matrix effects and self-absorption. It was reported that ANNs showed the potential to account for effects of chemical and physical matrices and overlapped lines (spectral matrix effects) when major elemental compositions of rock samples were measured [116]. While ANNs can in theory model matrix effects if a sufficiently rich database is used, it has been reported that improvements in the accuracy can be achieved by including temperature and electron density, which are considered in CF-LIBS, as additional inputs together with spectral data [117].

As for self-absorption, while several progressive methods for correction of self-absorption have been developed as described in previous sections, they often require detailed analysis of spectra. While the effects of self-absorption can be limited in PLS by reducing their weights, ANNs can in principle account for these effects by modelling the non-linear relationship using a flexible statistical model. This characteristic contributes to show a good performance when the spectral regions are limited to the range where self-absorption lines are dominant. Sirven et al. [30, 110] first applied ANNs to LIBS signals for quantification of Cr in soil samples, and showed that ANNs have advantages over conventional calibration curves and PLS especially in taking into account non-linearity between spectral intensities and the concentrations due to self-absorption in the plasma.

While ANNs can model complex relations including self-absorption and matrix effects, one of the crucial problems for ANNs is that ANNs are prone to overfitting specific datasets. In order to avoid this, it is necessary to have large volumes of training, test and validation data. One approach that has been explored is to use small networks to reduce the flexibility of the models and also limit the regions of the spectra used in order to eliminate the effects of noise [118]. This can lead to efficient implementations with small training datasets [119]. Ferreira et al. [20] used wrapper [120], which is a method of feature selection from the whole spectra, so as to decrease the input data without discarding important information in the spectra. Data treatment is also important to construct an efficient model. Normalisation of datasets diminishes

ACCEPTED MANUSCRIPT

the effects of signal fluctuations, which leads to accuracy improvement [121]. Self-organization maps also have the potential to mitigate problems with overfitting, since they can be used to visualise the relation between compositions and signals by constructing a two-dimension map so that the constructed model can be easily interpreted [122]. It should be recognised however, that methods to reduce the size and complexity of the training datasets needed also may reduce the general applicability of ANNs and potentially limit their performance, and so further research is needed in this area.

5.3. Comparison of methods

Comparing PCR and PLS, a calibration model constructed using PLS is more efficient than PCR in general, since LVs are chosen by taking into account not only signals but also the elemental concentrations. However, Hasegawa [105] pointed out that systematic errors affect the accuracy of PLS models more than PCR models, and therefore case studies are needed to characterize the performances under different experimental constraints. With regard to PLS, it has two forms; PLS1 and PLS2. The concentrations of one element and multiple elements are included in the output in PLS1 and in PLS2, respectively [105]. Multi-elemental concentrations are calculated simultaneously in PLS2, while an independent model for each component is constructed in PLS1 in Ref. [109]. While PLS2 can include all compositional data in the model and predict them at the same time, it was empirically found that PLS1 shows better performance than PLS2 in Ref. [123]. This was because the error variances of concentrations must be normalised equally in the model, *i.e.*, the elements with large uncertainties in concentrations can affect those with small uncertainties.

The performance of multivariate regression analysis is often compared with univariate calibration and other multivariate regression analysis. Yaroshchyk et al. [124] analysed Fe contents in ore samples using PCR and PLS, demonstrating that PLS required a smaller number of LVs than PCR. Ayyalasomayajula et al. [125] compared univariate calibration, multiple linear regression, and PLS1 to determine the compositions of Al, Ca, Fe, Ni and Si in slurry sam-

ACCEPTED MANUSCRIPT

ples, and found that PLS1 showed better consistency compared to the other methods, while the error remained relatively large for Si even using PLS1. In Ref. [126], univariate calibration, PCR and PLS were compared to quantify plutonium oxide surrogate residues for the application to on-line monitoring of hazardous waste management. PLS had the best accuracy with RMSEC values of 0.05-2.93 %. Based on these studies, PLS in general shows marginally better performance than PCR and the model is constructed more efficiently with a smaller number of LVs.

As for the ability of ANNs to model matrix effects, Inakollu et al. [118] compared an ANN with conventional calibration curves for ratios of metal elements in Al based alloys. They input peaks of several elements to the ANN model and reported that the ANN generally showed better performance for Cr, with a RE of 1-8 % obtained by ANNs compared to a RE of 0.04-54 % obtained by calibration curves. Ag, Cu and Pb in Sn based alloys were also investigated by an ANN and conventional calibration curves, and the ANN showed improvement of the RE for Cu and Pb, from 53 to 96 % reduction, while the ANN was less accurate for Ag, with 2 times larger REs than ones obtained by calibration curves [121]. This might be because of fluctuations of intensity, and it is conceivable that ANN models are more robust to systematic relations such as self-absorption and matrix effects than random noise. Sirven et al. [110] showed the advantage of ANNs over calibration curves and PLS when self-absorbed lines are dominant in the input spectral data. D'Andrea et al. [127] compared the performance of an ANN to OPC-LIBS. OPC-LIBS gave more accurate results for Cu, Zn, Ti, and Pb in bronze samples. While it needs further investigation for generalisation to samples with complex matrices, it can be inferred that theory-based analysis, such as OPC-LIBS, would have an advantage for quantitative analysis for spectra with well-resolved peaks since error sources in the analytical processes are limited. When overlapping of peaks are significant or the number of matrices is large, statistical analysis can potentially solve the problems using a model which can take complexity into account.

ACCEPTED MANUSCRIPT

5.4. In-situ applications of multivariate regression analysis

PCR and PLS are often applied for in-situ applications, such as on-line monitoring of quality in industrial applications and on-site analysis in environment surveys. As for laboratory based works, PCR and PLS have been investigated for many kinds of samples, such as precious metals [109, 128], preservative-treated wood [129], plants [130], soil [33, 131, 132], and fertilizer [24]. Since the output is not limited to elemental concentrations in PLS, the alternative chemical attributes such as the whole ash contents in coal samples can be inferred, as demonstrated using PLS1 in Ref. [133]. Doucet et al. [134] quantified isotope ratios of U_{235}/U_{238} using PLS1 with a RE of 0.1-8 %, which was considered acceptable for the targeted in-situ application. While most research considers targets in air at atmospheric pressure, PLS has been applied in other environmental conditions, such as underwater measurements for deep-sea applications. In the Ref. [102], large shot-to-shot fluctuations seen in signals taken in water were corrected by segmenting the database by temperature, which contributed to the enhancement of accuracy with a 30 % reduction of RMSECV. The application of PLS to in-situ analysis of Martian rock compositions using "ChemCam", the LIBS device mounted on the Mars rover, "Curiosity", has been reported [7, 135]. Through investigations in a laboratory environment and on-site experiments [2, 23, 136, 137], PLS1 and PLS2 showed the comparable results for the major components of rocks with a RMSEP of ∼9 % among other multivariate methods, such as elastic net, least absolute shrinkage and selection operator, support vector regression and k-nearest neighbor regression [138, 139]. Further development of generic quantitative methods is ongoing, especially aiming at robust prediction of compositions of unknown targets, which is crucial for the application to Mars exploration [140]. Clegg et al. [141] combined different types of multivariate regression methods, the sub-model PLS approach, which is introduced in section 5.1.2, and independent component analysis, which is typically used for classification but used for regression in the study by constructing a univariate model using extracted scores, resulting in significant improvement of the accuracy compared to conventional PLS.

ACCEPTED MANUSCRIPT

So far ANNs have been applied to classification and identification of LIBS signals [142, 143, 144, 145, 146]. One interesting application of ANNs is selection of optimised experimental parameters with which all peaks express compromised maximum area values [147]. While not many studies of ANNs regarding quantification of solid samples have been published, El Haddad et al. [31, 28] showed the potential of ANNs for in-situ analysis of soils. Different elements in soil compositions were quantified using ANN models constructed from spectra obtained at a mining site, and values of REP from 14 to 20 % were obtained for Cu, Al, Ca and Fe when peak intensities of several elements were used as input [31]. When ANNs are applied to practical in-situ analysis, the models constructed should be thoroughly examined by checking differences of calibration and prediction errors with a large dataset of samples that are similar to targets for in-situ analysis, in order to avoid overfitting data.

6. Conclusions

The basic concepts and applications of conventional calibration curves, CF-LIBS and multivariate analysis (PCR, PLS and ANN) to LIBS measurements of solids have been described. Matrix effects and self-absorption are known to disturb the linear relation between peak intensities and the concentration of a certain element. While calibration curves can be applied to matrix matched samples, there are practical limitations for in-situ applications, in which unknown samples, often with complex matrices, are measured. Self-absorption of lines causes non-linearity of the regression model and is most often seen at higher concentrations with strong lines terminating at the ground state. In order to overcome these problems, many methods to correct matrix effects and self-absorption have been proposed, such as normalisation of peaks and COG. However, quantitative analysis of samples with complex matrices remains an unsolved challenge for samples with widely varying matrices, which has limited their application so far to in-situ analysis.

In CF-LIBS, physical and chemical matrix effects are compensated through

ACCEPTED MANUSCRIPT

the basic physical model of plasma emission described by the Boltzmann distribution law and Saha equation under certain model assumptions. While self-absorption has in the past been one of the major limiting factors in the accuracy of CF-LIBS, several methods to correct for its effects have now been developed and significant progress has been made to improve the accuracy of quantitative analysis using LIBS. However, the requirements to detect the peaks of all elements and perform detailed analysis of these peaks requires significant prior knowledge of the target and is only practical in situations where the targets have relatively simple compositions. While this is not a problem for measurements of metallic alloys with some prior knowledge of the type of target being measured, these points limit the applications of CF-LIBS in situations where prior knowledge of the target cannot be reasonably assumed, such as in-situ measurements of natural targets, e. g., rocks or sediments in geological surveys and environmental pollution monitoring.

PCR and PLS express a linear relation, where only information which is linearly related to concentrations is isolated and extracted. Since they refer to the entire spectral information including peaks of the elements that compose the matrix and weight each region depending on its contribution to the linear relation, spectral, physical and chemical matrix effects can be taken into account in the model. While non-linear effects of self-absorption are in theory discarded from PCs and LVs, in practise, self-absorption effects can still influence the results and increase uncertainty and so spectral regions where self-absorption lines are not dominant should be used to improve accuracy. PLS has been applied in many studies for quantification of solids, especially in complicated in-situ applications such as soil analysis and planetary exploration.

ANNs can model any function including both linear and non-linear relationships, given a sufficient number of nodes and layers and a rich training dataset. So far, research applying ANNs to quantitative analysis of solid samples remain limited, although some works demonstrated that matrix effects and self-absorption are successfully modelled using ANNs. However, since overfitting is a serious problem for ANNs, models need to be constructed with a large

ACCEPTED MANUSCRIPT

dataset of samples and examined by thorough calibration and validation trials.

Since LIBS signals are obtained through observation of the transient emissions of a small plasma that is often unstable, the relation between peak intensity and the concentration of an element can be complex. For in-situ applications, the experimental environment cannot be controlled and so these effects cannot realistically be avoided. The methods introduced in this review either isolate and extract linear relations, or correct or express non-linear effects. From a number of studies investigating the use of LIBS to quantify the composition of solids, it can be inferred that theory-based methods are most effective for samples with relatively simple matrices, such as metal alloys, since these methods can consider specific sources of signal deformation and account for these separately using appropriate physical models. For samples with complex matrices and spectra, such as soils and rocks, accounting for a broad range of processes acting on a large number of peaks becomes impractical and statistical methods that can flexibly absorb the effects of various complicated forms of signal deformation can more effectively identify correlations between the features of the spectra and the concentration of the samples.

A number of different techniques are being investigated following the rapid progress in techniques for computational analysis. This is expected to be reflected in a further advance of quantitative techniques for target composition analysis using LIBS. As seen in this review, quantitative multivariate analysis using LIBS signals have recently been widely recognized in analytical chemistry as an important addition to more classical methods for quantification. In future studies, accuracy should be clearly described using common figures of merit, such as the NRMSE, in order that different methods can be compared for different experimental setups. By allowing direct comparison of analytical performances, development from different fields, e. g., computer science, spectroscopy, analytical chemistry and applied engineering, can be shared and this will accelerate the progress and the acceptance of LIBS for quantitative in-situ analysis.

ACCEPTED MANUSCRIPT

[1] J. Rakovský, P. Čermák, O. Musset, P. Veis, A review of the development of portable laser induced breakdown spectroscopy and its applications, Spectrochim. Acta Part B At. Spectrosc. 101 (2014) 269–287.

[2] J. M. Tucker, M. D. Dyar, M. W. Schaefer, S. M. Clegg, R. C. Wiens, Optimization of laser-induced breakdown spectroscopy for rapid geochemical analysis, Chem. Geol. 277 (2010) 137–148.

[3] D. Anglos, S. Couris, C. Fotakis, Laser diagnostics of painted artworks: laser-induced breakdown spectroscopy in pigment identification, Appl. Spectrosc. 51 (1997) 1025–1030.

[4] R. Noll, C. Fricke-Begemann, M. Brunk, S. Connemann, C. Meinhardt, M. Scharun, V. Sturm, J. Makowe, C. Gehlen, Laser-induced breakdown spectroscopy expands into industrial applications, Spectrochim. Acta Part B At. Spectrosc. 93 (2014) 41–51.

[5] F. J. Fortes, J. J. Laserna, The development of fieldable laser-induced breakdown spectrometer: No limits on the horizon, Spectrochim. Acta Part B At. Spectrosc. 65 (2010) 975–990.

[6] A. Whitehouse, J. Young, I. Botheroyd, S. Lawson, C. Evans, J. Wright, Remote material analysis of nuclear power station steam generator tubes by laser-induced breakdown spectroscopy, Spectrochim. Acta Part B At. Spectrosc. 56 (2001) 821–830.

[7] R. C. Wiens, S. Maurice, B. Barraclough, M. Saccoccio, W. C. Barkley, J. F. Bell, S. Bender, J. Bernardin, D. Blaney, J. Blank, M. Bouyè, N. Bridges, N. Bultman, P. Caïs, R. C. Clanton, B. Clark, S. Clegg, A. Cousin, D. Cremers, A. Cros, L. DeFlores, D. Delapp, R. Dingler, C. D′Uston, M. Darby Dyar, T. Elliott, D. Enemark, C. Fabre, M. Flores, O. Forni, O. Gasnault, T. Hale, C. Hays, K. Herkenhoff, E. Kan, L. Kirkland, D. Kouach, D. Landis, Y. Langevin, N. Lanza, F. LaRocca, J. Lasue, J. Latino, D. Limonadi, C. Lindensmith, C. Little, N. Mangold,

ACCEPTED MANUSCRIPT

G. Manhes, P. Mauchien, C. McKay, E. Miller, J. Mooney, R. V. Morris, L. Morrison, T. Nelson, H. Newsom, A. Ollila, M. Ott, L. Pares, R. Perez, F. Poitrasson, C. Provost, J. W. Reiter, T. Roberts, F. Romero, V. Sautter, S. Salazar, J. J. Simmonds, R. Stiglich, S. Storms, N. Striebig, J.-J. Thocaven, T. Trujillo, M. Ulibarri, D. Vaniman, N. Warner, R. Waterbury, R. Whitaker, J. Witt, B. Wong-Swanson, The ChemCam Instrument Suite on the Mars Science Laboratory (MSL) Rover: Body Unit and Combined System Tests, Space Sci. Rev. 170 (2012) 167–227.

[8] B. Thornton, T. Takahashi, T. Sato, T. Sakka, A. Tamura, A. Matsumoto, T. Nozaki, T. Ohki, K. Ohki, Development of a deep-sea laser-induced breakdown spectrometer for in situ multi-element chemical analysis, Deep Sea Res. Part I Oceanogr. Res. Pap. 95 (2015) 20–36.

[9] F. J. Fortes, S. Guirado, a. Metzinger, J. J. Laserna, A study of underwater stand-off laser-induced breakdown spectroscopy for chemical analysis of objects in the deep ocean, J. Anal. At. Spectrom. 30 (2015) 1050–1056.

[10] R. Nyga, W. Neu, Double-pulse technique for optical emission spectroscopy of ablation plasmas of samples in liquids, Opt. Lett. 18 (1993) 747–749.

[11] A. D. Giacomo, A. D. Bonis, M. Dell′Aglio, O. De Pascale, R. Gaudiuso, S. Orlando, A. Santagata, G. S. Senesi, F. Taccogna, R. Teghil, Laser Ablation of Graphite in Water in a Range of Pressure from 1 to 146 atm Using Single and Double Pulse Techniques for the Production of Carbon Nanostructures, J. Phys. Chem. C 115 (2011) 5123–5130.

[12] A. D. Giacomo, M. Dell′Aglio, A. Casavola, G. Colonna, O. D. Pascale, M. Capitelli, Elemental chemical analysis of submerged targets by double-pulse laser-induced breakdown spectroscopy., Anal. Bioanal. Chem. 385 (2006) 303–311.

[13] V. Lazic, F. Colao, R. Fantoni, V. Spizzicchino, Laser-induced breakdown

ACCEPTED MANUSCRIPT

spectroscopy in water: Improvement of the detection threshold by signal processing, Spectrochim. Acta Part B At. Spectrosc. 60 (2005) 1002–1013.

[14] T. Takahashi, B. Thornton, T. Ura, Investigation of influence of hydrostatic pressure on double-pulse Laser-Induced Breakdown Spectroscopy for detection of Cu and Zn in submerged solids, Appl. Phys. Express 6 (2013) 042403.

[15] T. Sakka, H. Oguchi, S. Masai, K. Hirata, Y. H. Ogata, M. Saeki, H. Ohba, Use of a long-duration ns pulse for efficient emission of spectral lines from the laser ablation plume in water, Appl. Phys. Lett. 88 (2006) 061120.

[16] B. Thornton, T. Ura, Effects of pressure on the optical emissions observed from solids immersed in water using a single pulse laser, Appl. Phys. Express 4 (2011) 022702.

[17] D. W. Hahn, N. Omenetto, Laser-induced breakdown spectroscopy (LIBS), part I: review of basic diagnostics and plasma-particle interactions: still-challenging issues within the analytical plasma community, Appl. Spectrosc. 64 (2010) 335–366.

[18] A. S. Eppler, D. A. Cremers, D. D. Hickmott, M. J. Ferris, A. C. Koskelo, Matrix effects in the detection of Pb and Ba in soils using laser-induced breakdown spectroscopy, Appl. Spectrosc. 50 (1996) 1175–1181.

[19] D. A. Cremers, L. J. Radziemski, History and fundamentals of LIBS, in: A. W. Miziolek, V. Palleschi, I. Schechter (Eds.), Laser-Induced Breakdown Spectroscopy, Cambridge University Press, New York, 2006.

[20] E. C. Ferreira, D. M. B. P. Milori, E. J. Ferreira, R. M. Da Silva, L. Martin-Neto, Artificial neural network for Cu quantitative determination in soil using a portable Laser Induced Breakdown Spectroscopy system, Spectrochim. Acta Part B At. Spectrosc. 63 (2008) 1216–1220.

ACCEPTED MANUSCRIPT

[21] D. A. Cremers, L. J. Radziemski, Basics of the LIBS Plasma, in: Laser-Induced Breakdown Spectroscopy, John Wiley & Sons Ltd., England, 2006.

[22] J. M. Mermet, Calibration in atomic spectrometry: A tutorial review dealing with quality criteria, weighting procedures and possible curvatures, Spectrochim. Acta Part B At. Spectrosc. 65 (2010) 509–523.

[23] S. M. Clegg, E. Sklute, M. D. Dyar, J. E. Barefield, R. C. Wiens, Multivariate analysis of remote laser-induced breakdown spectroscopy spectra using partial least squares, principal component analysis, and related techniques, Spectrochim. Acta Part B At. Spectrosc. 64 (2009) 79–88.

[24] S. Yao, J. Lu, J. Li, K. Chen, M. Dong, Multi-elemental analysis of fertilizer using laser-induced breakdown spectroscopy coupled with partial least squares regression, J. Anal. At. Spectrom. 25 (2010) 1733–1738.

[25] P. Pořízka, a. Demidov, J. Kaiser, J. Keivanian, I. Gornushkin, U. Panne, J. Riedel, Laser-induced breakdown spectroscopy for in situ qualitative and quantitative analysis of mineral ores, Spectrochim. Acta Part B At. Spectrosc. 101 (2014) 155–163.

[26] B. Praher, V. Palleschi, R. Viskup, J. Heitz, J. D. Pedarnig, Calibration free laser-induced breakdown spectroscopy of oxide materials, Spectrochim. Acta Part B At. Spectrosc. 65 (2010) 671–679.

[27] J. El Haddad, D. Bruyère, A. Ismaël, G. Gallou, V. Laperche, K. Michel, L. Canioni, B. Bousquet, Application of a series of artificial neural networks to on-site quantitative analysis of lead into real soil samples by laser induced breakdown spectroscopy, Spectrochim. Acta Part B At. Spectrosc. 97 (2014) 57–64.

[28] J. El Haddad, L. Canioni, B. Bousquet, Good practices in LIBS analysis: Review and advices, Spectrochim. Acta Part B At. Spectrosc. 101 (2014) 171–182.

ACCEPTED MANUSCRIPT

[29] A. Pichahchy, D. Cremers, M. Ferris, Elemental analysis of metals under water using laser-induced breakdown spectroscopy, Spectrochim. Acta Part B At. Spectrosc. 52 (1997) 25–39.

[30] J. B. Sirven, B. Bousquet, L. Canioni, L. Sarger, Laser-induced breakdown spectroscopy of composite samples: Comparison of advanced chemometrics methods, Anal. Chem. 78 (2006) 1462–1469.

[31] J. El Haddad, M. Villot-Kadri, A. Ismaël, G. Gallou, K. Michel, D. Bruyère, V. Laperche, L. Canioni, B. Bousquet, Artificial neural network for on-site quantitative analysis of soils using laser induced breakdown spectroscopy, Spectrochim. Acta Part B At. Spectrosc. 79-80 (2013) 51–57.

[32] E. Tognoni, G. Cristoforetti, S. Legnaioli, V. Palleschi, Calibration-Free Laser-Induced Breakdown Spectroscopy: State of art, Spectrochim. Acta Part B 65 (2010) 1–14.

[33] N. Yang, N. S. Eash, J. Lee, M. Z. Martin, Y.-S. Zhang, F. R. Walker, J. E. Yang, Multivariate analysis of Laser-Induced Breakdown Spectroscopy spectra of soil samples, Soil Sci. 175 (2010) 447–452.

[34] Q. Sun, M. Tran, B. W. Smith, J. D. Winefordner, Determination of Mn and Si in iron ore by laser-induced breakdown spectroscopy, Anal. Chim. Acta 413 (2000) 187–195.

[35] F. Capitelli, F. Colao, M. R. Provenzano, R. Fantoni, G. Brunetti, N. Senesi, Determination of heavy metals in soils by Laser Induced Breakdown Spectroscopy, Geoderma 106 (2002) 45–62.

[36] K. J. Grant, G. L. Paul, J. A. O′nell, Quantitative elemental analysis of iron ore by Laser-Induced Breakdown Spectroscopy, Appl. Spectrosc. 45 (1991) 3–7.

[37] E. Tognoni, V. Palleschi, M. Corsi, G. Cristoforetti, N. Omenetto, I. Gornushkin, B. W. Smith, J. D. Winefordner, From sample to signal in laser-

ACCEPTED MANUSCRIPT

induced breakdown spectroscopy: a complex route to quantitative analysis, Cambridge University Press, New York, 2006.

[38] M. Corsi, G. Cristoforetti, V. Palleschi, A. Salvetti, E. Tognoni, A fast and accurate method for the determination of precious alloys caratage by Laser Induced Plasma Spectroscopy, Eur. Phys. J. D-Atomic, Mol. Opt. Plasma Phys. 13 (2001) 373–377.

[39] L. Barrette, S. Turmel, On-line iron-ore slurry monitoring for real-time process control of pellet making processes using laser-induced breakdown spectroscopy: Graphitic vs. total carbon detection, Spectrochim. Acta Part B At. Spectrosc. 56 (2001) 715–723.

[40] K. H. Lepore, C. I. Fassett, E. A. Breves, S. Byrne, S. Giguere, T. Boucher, J. M. Rhodes, M. Vollinger, C. H. Anderson, R. W. Murray, M. D. Dyar, Matrix effects in quantitative analysis of Laser-Induced Breakdown Spectroscopy (LIBS) of rock powders doped with Cr, Mn, Ni, Zn, and Co, Applied Spectroscopy 71 (4) (2017) 600–625.

[41] M. Robson, D. M. B. P. Milori, E. C. Ferreira, E. J. Ferreira, F. J. Krug, L. Martin-Neto, Total carbon measurement in whole tropical soil sample, Spectrochimica Acta Part B: Atomic Spectroscopy 63 (2008) 1221–1224.

[42] S. Rosenwasser, G. Asimellis, B. Bromley, R. Hazlett, J. Martin, T. Pearce, A. Zigler, Development of a method for automated quantitative analysis of ores using LIBS, Spectrochim. Acta B 56 (2001) 707–714.

[43] J. M. Anzano, M. A. Villoria, A. Ruíz-Medina, R. J. Lasheras, Laser-induced breakdown spectroscopy for quantitative spectrochemical analysis of geological materials: Effects of the matrix and simultaneous determination, Anal. Chim. Acta 575 (2006) 230–235.

[44] R. Barbini, F. Colao, R. Fantoni, a. Palucci, S. Ribezzo, H. van der Steen, M. Angelone, Semi-quantitative time resolved LIBS measurements, Appl. Phys. B Lasers Opt. 65 (1997) 101–107.

ACCEPTED MANUSCRIPT

[45] W. B. Barnett, Theoretical principles of internal standardization in analytical emission spectroscopy, Sectrochimica Acta 23 (1968) 643–664.

[46] T. Sakka, H. Yamagata, H. Oguchi, K. Fukami, Y. H. Ogata, Emission spectroscopy of laser ablation plume: Composition analysis of a target in water, Appl. Surf. Sci. 255 (2009) 9576–9580.

[47] R. S. Harmon, F. C. De Lucia, a. W. Miziolek, K. L. McNesby, R. a. Walters, P. D. French, Laser-induced breakdown spectroscopy (LIBS) - an emerging field-portable sensor technology for real-time, in-situ geochemical and environmental analysis, Geochemistry Explor. Environ. Anal. 5 (2005) 21–28.

[48] J. Vrenegor, R. Noll, V. Sturm, Investigation of matrix effects in laser-induced breakdown spectroscopy plasmas of high-alloy steel for matrix and minor elements, Spectrochim. Acta Part B At. Spectrosc. 60 (2005) 1083–1091.

[49] V. Lazic, F. Colao, R. Fantoni, V. Spizzichino, S. Jovicevic, Underwater sediment analyses by laser induced breakdown spectroscopy and calibration procedure for fluctuating plasma parameters, Spectrochim. Acta Part B At. Spectrosc. 62 (2007) 30–39.

[50] B. Sallé, J.-L. Lacour, P. Mauchien, P. Fichet, S. Maurice, G. Manhès, Comparative study of different methodologies for quantitative rock analysis by Laser-Induced Breakdown Spectroscopy in a simulated Martian atmosphere, Spectrochim. Acta Part B At. Spectrosc. 61 (2006) 301–313.

[51] V. Margetic, K. Niemax, R. Hergenröder, A study of non-linear calibration graphs for brass with femtosecond laser-induced breakdown spectroscopy, Spectrochimica Acta - Part B Atomic Spectroscopy 56 (2001) 1003–1010.

[52] C. Chaléard, P. Mauchien, N. Andre, J. Uebbing, J. L. Lacour, C. Geertsen, Correction of matrix effects in quantitative elemental analysis with

ACCEPTED MANUSCRIPT

laser ablation optical emission spectrometry, J. Anal. At. Spectrom. 12 (1997) 183–188.

[53] L. Xu, V. Bulatov, V. V. Gridin, I. Schechter, Absolute analysis of particulate materials by laser-induced breakdown spectroscopy, Analytical Chemistry 69 (1997) 2103–2108.

[54] S. I. Gornushkin, I. B. Gornushkin, J. M. Anano, B. W. Smith, J. D. Winefordner, Effective normalization technique for correction of matrix effects in laser-induced breakdown spectroscopy detection of magnesium in powdered samples, Appl. Spectrosc. 56 (2002) 433–436.

[55] U. Panne, C. Haisch, M. Clara, R. Niessner, Analysis of glass and glass melts during the vitrification process of fly and bottom ashes by laser-induced plasma spectroscopy. Part I: Normalization and plasma diagnostics, Spectrochim. Acta Part B At. Spectrosc. 53 (1998) 1957–1968.

[56] C. Davies, H. Telle, D. Montgomery, R. Corbett, Quantitative analysis using remote laser-induced breakdown spectroscopy (LIBS), Spectrochim. Acta Part B At. Spectrosc. 50 (1995) 1059–1075.

[57] F. Bredice, F. O. Borges, H. Sobral, M. Villagran-Muniz, H. O. Di Rocco, G. Cristoforetti, S. Legnaioli, V. Palleschi, L. Pardini, a. Salvetti, E. Tognoni, Evaluation of self-absorption of manganese emission lines in Laser Induced Breakdown Spectroscopy measurements, Spectrochim. Acta Part B At. Spectrosc. 61 (2006) 1294–1303.

[58] F. Hilbk-kortenbruck, R. Noll, P. Wintjens, Analysis of heavy metals in soils using laser-induced breakdown spectrometry combined with laser-induced fluorescence, Spectrochim. Acta Part B At. Spectrosc. 56 (2001) 933–945.

[59] I. Gornushkin, J. Anzano, L. King, B. Smith, N. Omenetto, J. Winefordner, Curve of growth methodology applied to laser-induced plasma

ACCEPTED MANUSCRIPT

emission spectroscopy, Spectrochim. Acta Part B At. Spectrosc. 54 (1999) 491–503.

[60] C. Aragón, J. Bengoechea, J. A. Aguilera, Influence of the optical depth on spectral line emission from laser-induced plasmas, Spectrochimica Acta - Part B Atomic Spectroscopy 56 (2001) 619–628.

[61] C. Aragón, F. Peñalba, J. A. Aguilera, Curves of growth of neutral atom and ion lines emitted by a laser induced plasma, Spectrochimica Acta - Part B Atomic Spectroscopy 60 (2005) 879–887.

[62] M. Kuzuya, T. Mikami, O. Mikami, Improvement of analysis precision of laser microprobe analyser by correcting self-absorption, J. Spectrosc. Soc. Japan 36 (1987) 123–125.

[63] R. D. Cowan, G. H. Dieke, Self-absorption of spectrum lines, Rev. Mod. Phys. 20 (1948) 418–456.

[64] V. Lazic, R. Barbini, F. Colao, R. Fantoni, A. Palucci, Self-absorption model in quantitative laser induced breakdown spectroscopy measurements on soils and sediments, Spectrochim. Acta Part B At. Spectrosc. 56 (2001) 807–820.

[65] H. Y. Moon, K. K. Herrera, N. Omenetto, B. W. Smith, J. D. Winefordner, On the usefulness of a duplicating mirror to evaluate self-absorption effects in laser induced breakdown spectroscopy, Spectrochim. Acta Part B At. Spectrosc. 64 (2009) 702–713.

[66] G. Cristoforetti, E. Tognoni, Calculation of elemental columnar density from self-absorbed lines in laser-induced breakdown spectroscopy: A resource for quantitative analysis, Spectrochimica Acta - Part B Atomic Spectroscopy 79-80 (2013) 63–71.

[67] A. Ciucci, M. Corsi, V. Palleschi, S. Rastelli, A. Salvetti, E. Tognoni, New procedure for quantitative elemental analysis by Laser-Induced Plasma Spectroscopy, Appl. Spectrosc. 53 (1999) 960–964.

ACCEPTED MANUSCRIPT

[68] E. Tognoni, G. Cristoforetti, S. Legnaioli, V. Palleschi, Calibration-free laser-induced breakdown spectroscopy: state of the art, Spectrochim. Acta Part B At. Spectrosc. 65 (2010) 1–14.

[69] R. W. P. McWhirter, Spectral intensities, in: R. H. Huddlestone, S. L. Leonard (Eds.), Plasma diagnostic techniques, Academic Press, New York, 1965, pp. 201–264.

[70] G. Cristoforetti, a. De Giacomo, M. Dell′Aglio, S. Legnaioli, E. Tognoni, V. Palleschi, N. Omenetto, Local thermodynamic equilibrium in Laser-Induced Breakdown Spectroscopy: Beyond the McWhirter criterion, Spectrochim. Acta Part B At. Spectrosc. 65 (2010) 86–95.

[71] D. W. Hahn, N. Omenetto, Laser-induced breakdown spectroscopy (LIBS), part II: review of instrumental and methodological approaches to material analysis and applications to different fields., Appl. Spectrosc. 66 (2012) 347–419.

[72] M. L. Shah, a. K. Pulhani, G. P. Gupta, B. M. Suri, Quantitative elemental analysis of steel using calibration-free laser-induced breakdown spectroscopy, Appl. Opt. 51 (2012) 4612–4621.

[73] L. Fornarini, F. Colao, R. Fantoni, V. Lazic, V. Spizzicchino, Calibration analysis of bronze samples by nanosecond laser induced breakdown spectroscopy: A theoretical and experimental approach, Spectrochim. Acta Part B At. Spectrosc. 60 (2005) 1186–1201.

[74] E. Tognoni, G. Cristoforetti, S. Legnaioli, V. Palleschi, A. Salvetti, M. Mueller, U. Panne, I. Gornushkin, A numerical study of expected accuracy and precision in Calibration-Free Laser-Induced Breakdown Spectroscopy in the assumption of ideal analytical plasma, Spectrochim. Acta Part B At. Spectrosc. 62 (2007) 1287–1302.

[75] K. K. Herrera, E. Tognoni, N. Omenetto, B. W. Smith, J. D. Winefordner, Semi-quantitative analysis of metal alloys, brass and soil samples by

ACCEPTED MANUSCRIPT

calibration-free laser-induced breakdown spectroscopy: recent results and considerations, J. Anal. At. Spectrom. 24 (2009) 413–425.

[76] V. S. Burakov, V. V. Kiris, P. A. Naumenkov, S. N. Raikov, Calibration-free laser spectral analysis of glasses and copper alloys, Journal of Applied Spectroscopy 71 (2004) 740–746.

[77] M. Horňáčková, J. Plavčan, Z. Grolmusová, P. Konečný, I. Holický, P. Veis, Laser induced breakdown spectroscopy of geological samples with different homogeneity, in: 31st ICPIG, Granada, Spain, 2013, pp. 6–9.

[78] F. Colao, R. Fantoni, V. Lazic, A. Paolini, F. Fabbri, G. G. Ori, L. Marinangeli, A. Baliva, Investigation of LIBS feasibility for in situ planetary exploration: An analysis on Martian rock analogues, Planet. Space Sci. 52 (2004) 117–123.

[79] I. Borgia, L. M. Burgio, M. Corsi, R. Fantoni, V. Palleschi, A. Salvetti, M. C. Squarcialupi, E. Tognoni, Self-calibrated quantitative elemental analysis by laser-induced plasma spectroscopy: application to pigment analysis, J. Cult. Herit. 1 (2000) S281–S286.

[80] M. Corsi, G. Cristoforetti, M. Hidalgo, S. Legnaioli, V. Palleschi, A. Salvetti, E. Tognoni, C. Vallebona, Application of laser-induced breakdown spectroscopy technique to hair tissue mineral analysis, Appl. Opt. 42 (2003) 6133–6137.

[81] W. Lei, V. Motto-Ros, M. Boueri, Q. Ma, D. Zhang, L. Zheng, H. Zeng, J. Yu, Time-resolved characterization of laser-induced plasma from fresh potatoes, Spectrochim. Acta Part B At. Spectrosc. 64 (2009) 891–898.

[82] S. Pandhija, N. K. Rai, a. K. Rai, S. N. Thakur, Contaminant concentration in environmental samples using LIBS and CF-LIBS, Appl. Phys. B 98 (2009) 231–241.

ACCEPTED MANUSCRIPT

[83] V. K. Singh, V. Singh, A. K. Rai, S. N. Thakur, P. K. Rai, J. P. Singh, Quantitative analysis of gallstones using laser-induced breakdown spectroscopy, Appl. Opt. 47 (2008) G38–G47.

[84] J. Hermann, C. Gerhard, E. Axente, C. Dutouquet, Comparative investigation of laser ablation plumes in air and argon by analysis of spectral line shapes: Insights on calibration-free laser-induced breakdown spectroscopy, Spectrochimica Acta - Part B Atomic Spectroscopy 100 (2014) 189–196.

[85] M. Corsi, G. Cristoforetti, M. Giuffrida, M. Hidalgo, S. Legnaioli, V. Palleschi, A. Salvetti, E. Tognoni, C. Vallebona, Three-dimensional analysis of laser induced plasmas in single and double pulse configuration, Spectrochimica Acta - Part B Atomic Spectroscopy 59 (2004) 723–735.

[86] J. A. Aguilera, C. Aragón, Characterization of a laser-induced plasma by spatially resolved spectroscopy of neutral atom and ion emissions. Comparison of local and spatially integrated measurements, Spectrochimica Acta - Part B Atomic Spectroscopy 59 (2004) 1861–1876.

[87] V. Bulatov, R. Krasniker, I. Schechter, Study of matrix effects in laser plasma spectroscopy by combined multifiber spatial and temporal resolutions, Analytical Chemistry 70 (1998) 5302–5311.

[88] I. B. Gornushkin, S. V. Shabanov, S. Merk, E. Tognoni, U. Panne, Effects of non-uniformity of laser induced plasma on plasma temperature and concentrations determined by the Boltzmann plot method: implications from plasma modeling, Journal of Analytical Atomic Spectrometry 25 (2010) 1643–1653.

[89] M. Gagean, J. Mermet, Study of laser ablation of brass materials using inductively coupled plasma atomic emission spectrometric detection, Spectrochimica Acta Part B: Atomic Spectroscopy 53 (1998) 581–591.

ACCEPTED MANUSCRIPT

[90] V. N. Lednev, S. M. Pershin, Plasma stoichiometry correction method in laser-induced breakdown spectroscopy, Laser Phys. 18 (2008) 850–854.

[91] T. Takahashi, B. Thornton, K. Ohki, T. Sakka, Calibration-free analysis of immersed brass alloys using long-ns-duration pulse laser-induced breakdown spectroscopy with and without correction for nonstoichiometric ablation, Spectrochim. Acta Part B At. Spectrosc. 111 (2015) 8–14.

[92] D. Bulajic, M. Corsi, G. Cristoforetti, S. Legnaioli, V. Palleschi, A. Salvetti, E. Tognoni, A procedure for correcting self-absorption in calibration free-laser induced breakdown spectroscopy, Spectrochim. Acta Part B At. Spectrosc. 57 (2002) 339–353.

[93] C. Aragón, J. A. Aguilera, CSigma graphs: A new approach for plasma characterization in laser-induced breakdown spectroscopy, Journal of Quantitative Spectroscopy and Radiative Transfer 149 (2014) 90–102.

[94] C. Aragón, J. Aguilera, Quantitative analysis by laser-induced breakdown spectroscopy based on generalized curves of growth, Spectrochimica Acta Part B: Atomic Spectroscopy 110 (2015) 124–133.

[95] L. Sun, H. Yu, Correction of self-absorption effect in calibration-free laser-induced breakdown spectroscopy by an internal reference method, Talanta 79 (2009) 388–395.

[96] H. Amamou, A. Bois, B. Ferhat, R. Redon, B. Rossetto, P. Matheron, Correction of self-absorption spectral line and ratios of transition probabilities for homogeneous and LTE plasma, Journal of Quantitative Spectroscopy and Radiative Transfer 75 (2002) 747–763.

[97] A. M. El Sherbini, T. M. El Sherbini, H. Hegazy, G. Cristoforetti, S. Legnaioli, V. Palleschi, L. Pardini, A. Salvetti, E. Tognoni, Evaluation of self-absorption coefficients of aluminum emission lines in laser-induced breakdown spectroscopy measurements, Spectrochimica Acta - Part B Atomic Spectroscopy 60 (2005) 1573–1579.

ACCEPTED MANUSCRIPT

[98] F. Bredice, F. O. Borges, H. Sobral, M. Villagran-Muniz, H. O. Di Rocco, G. Cristoforetti, S. Legnaioli, V. Palleschi, A. Salvetti, E. Tognoni, Measurement of Stark broadening of Mn I and Mn II spectral lines in plasmas used for Laser-Induced Breakdown Spectroscopy, Spectrochimica Acta - Part B Atomic Spectroscopy 62 (11) (2007) 1237–1245.

[99] F. O. Bredice, H. O. D. I. Rocco, H. M. Sobral, M. Villagránmuniz, V. Palleschi, A new method for determination of self-absorption coefficients of emission lines in laser-induced breakdown spectroscopy experiments, Applied Spectroscopy 64 (2010) 320–323.

[100] R. Gaudiuso, M. Dell'Aglio, O. De Pascale, A. Santagata, A. De Giacomo, Laser-induced plasma analysis of copper alloys based on local thermodynamic equilibrium: An alternative approach to plasma temperature determination and archeometric applications, Spectrochimica Acta - Part B Atomic Spectroscopy 74-75 (2012) 38–45.

[101] G. Cavalcanti, D. Teixeira, S. Legnaioli, G. Lorenzetti, L. Pardini, V. Palleschi, One-point calibration for calibration-free laser-induced breakdown spectroscopy quantitative analysis, Spectrochim. Acta Part B At. Spectrosc. 87 (2013) 51–56.

[102] T. Takahashi, B. Thornton, T. Sato, T. Ohki, K. Ohki, T. Sakka, Temperature based segmentation of laser-induced plasmas for quantitative compositional analysis of brass alloys submerged in water, Spectrochim. Acta Part B At. Spectrosc. 124 (2016) 87–93.

[103] N. Labbé, I. M. Swamidoss, N. André, M. Z. Martin, T. M. Young, T. G. Rials, Extraction of information from laser-induced breakdown spectroscopy spectral data by multivariate analysis, Appl. Opt. 47 (2008) G158–G165.

[104] J. M. Andrade-Garda, A. Carlosena-Zubieta, R. Boque-Marti, J. Ferre-Baldrich, Partial least-squares regression, in: J. M. Andrade-Garda (Ed.),

ACCEPTED MANUSCRIPT

Basic chemometric techniques in atomic spectroscopy, The Royal Society of Chemistry, Cambridge, 2013, pp. 280–347.

[105] T. Hasegawa, Principal component regression and partial least squares modeling, in: J. M. Chalmers, P. R. Griffiths (Eds.), Handbook of Vibrational Spectroscopy, John Wiley & Sons, Ltd, 2002, pp. 2293–2312.

[106] P. Geladi, B. R. Kowalski, Partial least-squares regression: a tutorial, Anal. Chim. Acta 185 (1986) 1–17.

[107] D. Death, A. Cunningham, L. Pollard, Multi-element analysis of iron ore pellets by Laser-induced Breakdown Spectroscopy and Principal Components Regression, Spectrochim. Acta Part B At. Spectrosc. 63 (2008) 763–769.

[108] R. B. Anderson, S. M. Clegg, J. Frydenvang, R. C. Wiens, S. McLennan, R. V. Morris, B. Ehlmann, M. D. Dyar, Improved accuracy in quantitative laser-induced breakdown spectroscopy using sub-models, Spectrochimica Acta - Part B Atomic Spectroscopy 129 (2017) 49–57.

[109] J. Amador-Hernández, Partial least squares regression for problem solving in precious metal analysis by laser induced breakdown spectrometry, J. Anal. At. Spectrom. 15 (2000) 587–593.

[110] J. B. Sirven, B. Bousquet, L. Canioni, L. Sarger, Laser-induced breakdown spectroscopy of composite samples: Comparison of advanced chemometrics methods, Anal. Chem. 78 (2006) 1462–1469.

[111] J. M. Andrade-Garda, M. Gestal-Pose, F. A. Cedron-Santaeufemia, J. Dorado-De-La-Calle, M. P. Gomez-Carracedo, Multivariate regression using artificial neural networks and support vector machines, in: J. M. Andrade-Garda (Ed.), Basic chemometric techniques in atomic spectroscopy, The Royal Society of Chemistry, Cambridge, 2013, pp. 348–397.

[112] M. T. Hagan, H. B. Demuth, M. H. Beale, O. De Jesús, Neural network design, Vol. 20, PWS publishing company Boston, 1996.

ACCEPTED MANUSCRIPT

[113] A. K. Jain, J. Mao, Artificial Neural Network: A Tutorial, Computer 29 (1996) 31–44.

[114] G. Kateman, Neural networks in analytical chemistry?, Chemom. Intell. Lab. Syst. 19 (1993) 135–142.

[115] A. Koujelev, S.-L. Lui, Artificial Neural Networks for Material Identification , Mineralogy and Analytical Geochemistry Based on Laser-Induced Breakdown Spectroscopy, in: K. Suzuki (Ed.), Artificial Neural Networks - Industrial and control engineering applications, InTech, Shanghai, 2010, pp. 91–114.

[116] V. Motto-Ros, A. S. Koujelev, G. R. Osinski, A. E. Dudelzak, Quantitative multi-elemental laser-induced breakdown spectroscopy using artificial neural networks, J. Eur. Opt. Soc. Rapid Publ. 3 (2008) 08011.

[117] E. D′Andrea, S. Pagnotta, E. Grifoni, S. Legnaioli, G. Lorenzetti, V. Palleschi, B. Lazzerini, A hybrid calibration-free/artificial neural networks approach to the quantitative analysis of LIBS spectra, Appl. Phys. B 118 (2015) 353–360.

[118] P. Inakollu, T. Philip, A. K. Rai, F. Y. Yueh, J. P. Singh, A comparative study of laser induced breakdown spectroscopy analysis for element concentrations in aluminum alloy using artificial neural networks and calibration methods, Spectrochim. Acta Part B At. Spectrosc. 64 (2009) 99–104.

[119] F. Dieterle, S. Busche, G. Gauglitz, Different approaches to multivariate calibration of nonlinear sensor data, Analytical and bioanalytical chemistry 380 (2004) 383–396.

[120] R. Kohavi, G. H. John, Wrappers for feature subset selection, Artificial Intelligence 97 (1-2) (1997) 273–324.

ACCEPTED MANUSCRIPT

[121] S. Y. Oh, Laser induced breakdown spectroscopy: Investigation of line profiles, slurries and artificial neural network prediction, Mississippi State University, Mississippi, 2007, Ch. 6.

[122] S. Pagnotta, E. Grifoni, S. Legnaioli, M. Lezzerini, G. Lorenzetti, V. Palleschi, Comparison of brass alloys composition by laser-induced breakdown spectroscopy and self-organizing maps, Spectrochim. Acta Part B At. Spectrosc. 103-104 (2015) 70–75.

[123] D. M. Haaland, E. V. Thomas, Partial least-squares methods for spectral analyses. 1. Relation to other quantitative calibration methods and the extraction of qualitative information, Anal. Chem. 60 (1988) 1193–1202.

[124] P. Yaroshchyk, D. L. Death, S. J. Spencer, Comparison of principal components regression, partial least squares regression, multi-block partial least squares regression, and serial partial least squares regression algorithms for the analysis of Fe in iron ore using LIBS, J. Anal. At. Spectrom. 27 (2012) 92–98.

[125] K. K. Ayyalasomayajula, V. Dikshit, F. Y. Yueh, J. P. Singh, L. T. Smith, Quantitative analysis of slurry sample by laser-induced breakdown spectroscopy, Anal. Bioanal. Chem. 400 (2011) 3315–3322.

[126] M. M. Tripathi, K. E. Eseller, F.-Y. Yueh, J. P. Singh, Multivariate calibration of spectra obtained by Laser Induced Breakdown Spectroscopy of plutonium oxide surrogate residues, Spectrochim. Acta Part B At. Spectrosc. 64 (2009) 1212–1218.

[127] E. D'Andrea, S. Pagnotta, E. Grifoni, G. Lorenzetti, S. Legnaioli, V. Palleschi, B. Lazzerini, An artificial neural network approach to laser-induced breakdown spectroscopy quantitative analysis, Spectrochimica Acta - Part B Atomic Spectroscopy 99 (2014) 52–58.

[128] A. Jurado-López, M. D. L. De Castro, An atypical interlaboratory assay:

ACCEPTED MANUSCRIPT

Looking for an updated hallmark (-jewelry) method, Anal. Bioanal. Chem. 372 (2002) 109–114.

[129] M. Z. Martin, N. Labbé, T. G. Rials, S. D. Wullschleger, Analysis of preservative-treated wood by multivariate analysis of laser-induced breakdown spectroscopy spectra, Spectrochim. Acta Part B At. Spectrosc. 60 (2005) 1179–1185.

[130] J. W. B. Braga, L. C. Trevizan, L. C. Nunes, I. A. Rufini, D. Santos, F. J. Krug, Comparison of univariate and multivariate calibration for the determination of micronutrients in pellets of plant materials by laser induced breakdown spectrometry, Spectrochim. Acta Part B At. Spectrosc. 65 (2010) 66–74.

[131] R. Wisbrun, I. Schechter, R. Niessner, H. Schroeder, K. L. Kompa, Detector for Trace Elemental Analysis of Solid Environmental Samples by Laser Plasma Spectroscopy, Analytical Chemistry 66 (1994) 2964–2975.

[132] M. E. Essington, G. V. Melnichenko, M. A. Stewart, R. A. Hull, Soil Metals Analysis Using Laser-Induced Breakdown Spectroscopy (LIBS), Soil Sci. Soc. Am. J. 73 (2009) 1469.

[133] S. Yao, J. Lu, M. Dong, K. Chen, J. Li, J. Li, Extracting coal ash content from laser-induced breakdown spectroscopy (LIBS) spectra by multivariate analysis, Appl. Spectrosc. 65 (2011) 1197–1201.

[134] F. R. Doucet, G. Lithgow, R. Kosierb, P. Bouchard, M. Sabsabi, Determination of isotope ratios using Laser-Induced Breakdown Spectroscopy in ambient air at atmospheric pressure for nuclear forensics, J. Anal. At. Spectrom. 26 (2011) 536–541.

[135] P. Meslin, O. Gasnault, O. Forni, S. Schröder, A. Cousin, G. Berger, S. M. Clegg, J. Lasue, S. Maurice, V. Sautter, S. L. Mouélic, R. C. Wiens, C. Fabre, W. Goetz, D. Bish, N. Mangold, B. Ehlmann, N. Lanza,

ACCEPTED MANUSCRIPT

A. Harri, R. Anderson, E. Rampe, Soil Diversity and Hydration at Gale Crater, Mars 341 (2013) 1–10.

[136] R. B. Anderson, J. F. Bell, R. C. Wiens, R. V. Morris, S. M. Clegg, Clustering and training set selection methods for improving the accuracy of quantitative laser induced breakdown spectroscopy, Spectrochim. Acta Part B At. Spectrosc. 70 (2012) 24–32.

[137] R. Wiens, S. Maurice, J. Lasue, O. Forni, R. Anderson, S. Clegg, S. Bender, D. Blaney, B. Barraclough, A. Cousin, L. Deflores, D. Delapp, M. Dyar, C. Fabre, O. Gasnault, N. Lanza, J. Mazoyer, N. Melikechi, P.-Y. Meslin, H. Newsom, A. Ollila, R. Perez, R. Tokar, D. Vaniman, Pre-flight calibration and initial data processing for the ChemCam laser-induced breakdown spectroscopy instrument on the Mars Science Laboratory rover, Spectrochim. Acta Part B At. Spectrosc. 82 (2013) 1–27.

[138] M. D. Dyar, M. L. Carmosino, E. A. Breves, M. V. Ozanne, S. M. Clegg, R. C. Wiens, Comparison of partial least squares and lasso regression techniques as applied to laser-induced breakdown spectroscopy of geological samples, Spectrochim. Acta Part B At. Spectrosc. 70 (2012) 51–67.

[139] T. F. Boucher, M. V. Ozanne, M. L. Carmosino, M. D. Dyar, S. Mahadevan, E. a. Breves, K. H. Lepore, S. M. Clegg, A study of machine learning regression methods for major elemental analysis of rocks using laser-induced breakdown spectroscopy, Spectrochim. Acta Part B At. Spectrosc. 107 (2015) 1–10.

[140] S. Maurice, S. M. Clegg, R. C. Wiens, O. Gasnault, W. Rapin, O. Forni, A. Cousin, V. Sautter, N. Mangold, L. Le Deit, M. Nachon, R. B. Anderson, N. L. Lanza, C. Fabre, V. Payré, J. Lasue, P.-Y. Meslin, R. J. Léveillé, B. L. Barraclough, P. Beck, S. C. Bender, G. Berger, J. C. Bridges, N. T. Bridges, G. Dromart, M. D. Dyar, R. Francis, J. Frydenvang, B. Gondet, B. L. Ehlmann, K. E. Herkenhoff, J. R. Johnson, Y. Langevin, M. B.

ACCEPTED MANUSCRIPT

Madsen, N. Melikechi, J.-L. Lacour, S. Le Mouélic, E. Lewin, H. E. Newsom, A. M. Ollila, P. Pinet, S. Schröder, J.-B. Sirven, R. L. Tokar, M. J. Toplis, C. D'Uston, D. T. Vaniman, A. R. Vasavada, ChemCam activities and discoveries during the nominal mission of the Mars Science Laboratory in Gale crater, Mars, J. Anal. At. Spectrom. 31 (2016) 863–889.

[141] S. M. Clegg, R. C. Wiens, R. Anderson, O. Forni, J. Frydenvang, J. Lasue, A. Cousin, V. Payré, T. Boucher, M. D. Dyar, S. M. McLennan, R. V. Morris, T. G. Graff, S. A. Mertzman, B. L. Ehlmann, I. Belgacem, H. Newsom, B. C. Clark, N. Melikechi, A. Mezzacappa, R. E. McInroy, R. Martinez, P. Gasda, O. Gasnault, S. Maurice, Recalibration of the Mars Science Laboratory ChemCam instrument with an expanded geochemical database, Spectrochimica Acta - Part B Atomic Spectroscopy 129 (2017) 64–85.

[142] S. Yoshino, T. Takahashi, B. Thornton, Towards in-situ chemical classification of seafloor deposits: Application of Neural Networks tounderwater Laser-induced breakdown spectroscopy, in: Oceans. 2017, IEEE, Aberdeen, Scotland, 2017, pp. 1–5.

[143] C. Bohling, K. Hohmann, D. Scheel, C. Bauer, W. Schippers, J. Burgmeier, U. Willer, G. Holl, W. Schade, All-fiber-coupled laser-induced breakdown spectroscopy sensor for hazardous materials analysis, Spectrochim. Acta Part B At. Spectrosc. 62 (2007) 1519–1527.

[144] S.-L. Lui, A. Koujelev, Accurate identification of geological samples using artificial neural network processing of laser-induced breakdown spectroscopy data, J. Anal. At. Spectrom. 26 (2011) 2419.

[145] G. Vítková, K. Novotný, L. Prokes, A. Hrdlička, J. Kaiser, J. Novotný, R. Malina, D. Prochazka, Fast identification of biominerals by means of stand-off laser-induced breakdown spectroscopy using linear discriminant analysis and artificial neural networks, Spectrochim. Acta Part B At. Spectrosc. 73 (2012) 1–6.

ACCEPTED MANUSCRIPT

[146] J. O. Caceres, S. Moncayo, J. D. Rosales, F. J. M. De Villena, F. C. Alvira, G. M. Bilmes, Application of laser-induced breakdown spectroscopy (LIBS) and neural networks to olive oils analysis, Applied Spectroscopy 67 (2013) 1064–1072.

[147] L. C. Nunes, G. A. da Silva, L. C. Trevizan, D. Santos Júnior, R. J. Poppi, F. J. Krug, Simultaneous optimization by neuro-genetic approach for analysis of plant materials by laser induced breakdown spectroscopy, Spectrochim. Acta Part B At. Spectrosc. 64 (2009) 565–572.

ACCEPTED MANUSCRIPT

ACCEPTED MANUSCRIPT

Graphical abstract

Calibration curve

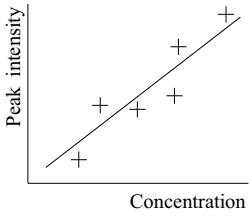

CF-LIBS

$$ln\frac{I_{s_{ij}}}{A_{s_{ij}}g_{s_i}} = -\frac{E_{s_i}}{k_B T} + ln\frac{FN_s}{U_s(T)}$$

$I_{s_{ij}}$: peak intensity; T: temperature; N_s: number density
$A_{s_{ij}}$: transition probability; g_{s_i}: statistical weight; E_{s_i}: excitation energy
k_B: Boltzmann constant; F: experimental parameter; $U_s(T)$: partition function

PCR

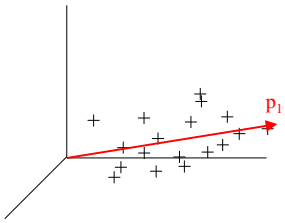

PLS

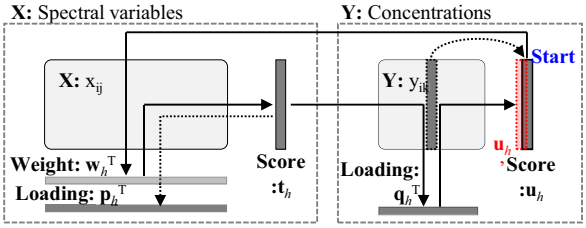

ANN

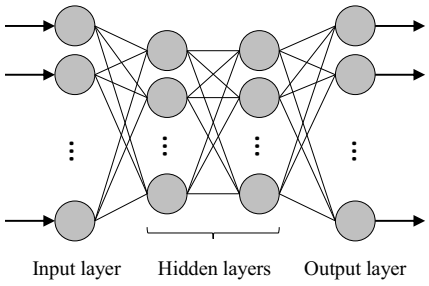

ACCEPTED MANUSCRIPT

Highlights

- Quantitative analytical methods with compensation for matrix and self-absorption effects for solid targets are reviewed.
- Figures of merit, methods, and their applications are described, especially focusing on in-situ applications.
- Accuracy comparison among different experimental setups and methods using common figures of merit is recommended, which will lead to further development of quantitative methods for in-situ LIBS.

ACCEPTED MANUSCRIPT